SCIENTIFIC REPORTS

OPEN

SUBJECT AREAS:
MECHANISMS OF DISEASE
ANTISENSE OLIGO
DRUG DELIVERY
RNA SPLICING

Received
18 March 2013

Accepted
21 June 2013

Published
22 July 2013

Correspondence and requests for materials should be addressed to S.I. (cishiura@mail.ecc.u-tokyo.ac.jp)

Ultrasound-enhanced delivery of Morpholino with Bubble liposomes ameliorates the myotonia of myotonic dystrophy model mice

Michinori Koebis[1], Tamami Kiyatake[1], Hiroshi Yamaura[1], Kanako Nagano[1], Mana Higashihara[2], Masahiro Sonoo[3], Yukiko Hayashi[4], Yoichi Negishi[5], Yoko Endo-Takahashi[5], Dai Yanagihara[1], Ryoichi Matsuda[1], Masanori P. Takahashi[6], Ichizo Nishino[4] & Shoichi Ishiura[1]

[1]Graduate School of Arts and Sciences, the University of Tokyo, Tokyo, Japan, [2]Division of Neurology, Department of Internal Medicine 3, National Defense Medical College, Saitama, Japan, [3]Department of Neurology, Teikyo University School of Medicine, Tokyo, Japan, [4]Department of Neuromuscular Research, National Institute of Neuroscience, National Center of Neurology and Psychiatry (NCNP), Tokyo, Japan, [5]Department of Drug Delivery and Molecular Biopharmaceutics, School of Pharmacy, Tokyo University of Pharmacy and Life Sciences, Tokyo, Japan, [6]Department of Neurology, Osaka University Graduate School of Medicine, Osaka, Japan.

Phosphorodiamidate morpholino oligonucleotide (PMO)-mediated control of the alternative splicing of the chloride channel 1 (*CLCN1*) gene is a promising treatment for myotonic dystrophy type 1 (DM1) because the abnormal splicing of this gene causes myotonia in patients with DM1. In this study, we optimised a PMO sequence to correct *Clcn1* alternative splicing and successfully remedied the myotonic phenotype of a DM1 mouse model, the *HSA*^{LR} mouse. To enhance the efficiency of delivery of PMO into *HSA*^{LR} mouse muscles, Bubble liposomes, which have been used as a gene delivery tool, were applied with ultrasound exposure. Effective delivery of PMO led to increased expression of Clcn1 protein in skeletal muscle and the amelioration of myotonia. Thus, PMO-mediated control of the alternative splicing of the *Clcn1* gene must be important target of antisense therapy of DM1.

Myotonic dystrophy type 1 (DM1) is caused by expansion of the CTG repeat in the 3′ untranslated region (UTR) of the *DMPK* gene[1–4]. Patients with DM1 show multi-systemic symptoms, including muscle wasting, muscle weakness, myotonia, cardiac conduction defect, cataracts, mental retardation and insulin resistance[5]. A patient, however, does not always present with all of these symptoms and the severity of the disease varies among individuals. Among the symptoms, myotonia is the most prominent and common phenotype of DM1: most patients feel muscle stiffness and difficulty in relaxing muscles soon after developing the disease.

The characteristic feature of the pathology of DM1 is the aberrant regulation of dozens of alternative splicing events, and some of the abnormal splicing events have been suggested to be involved in some of the symptoms[6–10]. Myotonic discharge is thought to be caused by the aberrant alternative splicing of the chloride channel 1 (*CLCN1*) gene[11,12]. In patients with DM1, extra exons from intron 6 are spliced into the *CLCN1* mRNA, leading to the appearance of a premature termination codon in the subsequent exon, degradation of the mRNA by nonsense-mediated decay and decreased expression of CLCN1 protein[11]. The idea that abnormal splicing of the *CLCN1* gene causes myotonia is strongly supported by the fact that the *CLCN1* gene is the only gene responsible for congenital myotonia, and the identification of multiple mutations in patients with the disease and their families[13]. Wheeler and his colleagues corrected the abnormal splicing of the *Clcn1* gene in a DM1 mouse model, the *HSA*^{LR} mouse, by using an antisense oligonucleotide (AON) and successfully alleviated the myotonic phenotype[14]. Thus, correction of the abnormally regulated splicing is a promising treatment for DM1.

An AON is a short, synthetic nucleic acid molecule with a sequence complementary to a target transcript. It can be used to manipulate an alternative splicing event: the AON that binds to the region around the target exon, specifically splice sites or splicing enhancer domains, physically blocks assembly of the spliceosome on the exon and induces exon skipping[15]. The efficacy of an AON is dependent on its half-life, affinity for its target RNA and *in*

vivo kinetics. A variety of AON molecules with 2′-*O* modifications and/or unnatural backbones have been developed to improve nuclease resistance and affinity for RNA[15]. Among them, Morpholino (also referred as phosphorodiamidate morpholino oligonucleotide [PMO]) is one of the most hopeful AONs. PMO has morpholine rings linked with phosphorodiamidate linkages in its backbone instead of deoxyribose and phosphodiester bonds. Due to its completely unnatural chemistry, PMO is hardly recognised by cellular nucleases. It has higher affinity for RNA than for DNA; the T_m value of a hybrid of PMO and RNA is much higher than that of DNA and RNA[16]. Several papers have reported the local and systemic administration of PMO to mice and dogs. For example, when a high dose of PMO (3 g/kg) was administrated intravenously into the *mdx* mouse, a mouse model of Duchenne muscular dystrophy, the PMO entered skeletal muscle without any assistive delivery reagent[17]. However, unlike mdx mice, muscle penetration of Evans Blue dye did not increase in HSA^{LR} and wild-type mice[18], which indicated a physical barrier to PMO uptake should be grater in HSA^{LR} than in *mdx*. In preceding reports on PMO treatment in HSA^{LR}, intravenous administration of CAG25 PMO led no detectable improvements in *Serca1* splicing in HSA^{LR} mice[19], and even when PMO was injected intramuscularly its uptake was limited to the needle track[14]. In these studies, they used electroporation to administer unmodified PMO intramuscularly, so we investigated a less invasive PMO delivery method to develop PMO treatment for DM1.

Recently, ultrasound exposure has been used for the intracellular delivery of molecules such as dextran, plasmid DNA and siRNA. If ultrasound is sufficiently strong, it will generate microscopic vacuum bubbles in a solution by a process known as inertial cavitation. The bubbles immediately collapse, producing a shock wave, which is believed to transiently increase the permeability of cell membranes in the vicinity. Inertial cavitation is enhanced by using micro bubbles of echo-contrast gas. This method has been applied to gene delivery into various mouse tissues, including skeletal muscle, liver and tumour tissues[20–22]; however, introducing genes into deep tissues with microbubbles is difficult because of their size and instability. To overcome these problems, we previously developed a novel drug delivery reagent coined "Bubble liposomes", polyethylene glycol-modified liposomes (PEG liposomes) encapsulating echo-contrast gas[23]. Owing to the stability in serum and uniform microscopic size of PEG liposomes, we successfully delivered genes and siRNA into several tissues[24–28]. However, does the Bubble liposome-ultrasound delivery system efficiently deliver PMO into skeletal muscles in the HSA^{LR} mice? In this study, we examined the ability of the Bubble liposome-ultrasound system to deliver PMO into skeletal muscles of HSA^{LR} mice as a treatment for abnormal splicing.

We newly designed antisense PMOs targeting exon 7A of the *Clcn1* gene and delivered them into HSA^{LR} mice. The PMOs were successfully delivered into skeletal muscles by the Bubble liposome-ultrasound system, which decreased the inclusion of exon 7A *in vivo*. Furthermore, the injection of PMO ameliorated the myotonic phenotype of the model mice. Our results suggest that Bubble liposomes should be effective for delivering PMOs into muscle tissues and can be applied to PMO treatment of DM1.

Results

We first determined the optimal target sequence of the *Clcn1* pre-mRNA to promote skipping of exon 7A. To achieve this, we used a *Clcn1* minigene and examined its alternative splicing using a cell culture-based assay. The minigene contains the genomic region from exon 6 to exon 7 of the murine *Clcn1* gene. When it was transfected into COS-7 cells, approximately 50% of transcripts contained exon 7A (Fig. 1b, minigene only). To screen for an optimal AON sequence, we used 25-mer phosphorothioate 2′ *O*-methyl (PS2OMe) RNA, which can regulate alternative splicing by sterically preventing spliceosomal assembly, just like PMO. We examined PS2OMe RNA molecules that covered the whole of exon 7A (1–25, 26–50, 51–75 and 76–90) and the boundary of intron 6 and exon 7A (−10–15). We transfected the minigene together with the PS2OMe RNA into COS-7 cells and analysed the alternative splicing of the minigene. We found that −10–15 and 1–25 PS2OMe significantly reduced the rate of inclusion of exon 7A, with 1–25 PS2OMe being the most effective molecule (Fig. 1b).

Previously, we identified the 8 nt at the 5′ end of exon 7A as an exonic splicing enhancer (ESE) essential for basal inclusion of the exon[29]. Given that both −10–15 and 1–25 PS2OMe covered the ESE, and that 1–25 PS2OMe seemed to be more effective at excluding exon 7A, we speculated that another ESE (16–25) would be located in the region +16 to +25, and that 1–25 PS2OMe would not share it with −10–15 PS2OMe. To examine this possibility, we tested whether 16–40 PS2OMe enhanced normal splicing. 16–40 PS2OMe markedly reduced the rate of inclusion of exon 7A of the *Clcn1* minigene (Supplementary Fig. S1). As 26–50 PS2OMe did not change the alternative splicing, we conclude that the other ESE (16–25) is important for exon 7A inclusion. Thus, we used 1–25 AON, which targeted both ESEs, in subsequent experiments.

PS2OMe is highly resistant to nuclease-mediated degradation owing to its phosphorothioate linkages; however, it is still degraded slowly and releases monomers that have a toxic, free phosphorothioate group. In contrast, PMO is remarkably resistant to degradation and is not noxious. Therefore, we next investigated whether a PMO with the same sequence as 1–25 PS2OMe also improved the alternative splicing of exon 7A by using the cell culture-based splicing assay (Fig. 1c). The −11–14 PMO we used here had the same sequence as that Wheeler and his colleagues used in a previous study[14]. RT-PCR analysis showed that both 1–25 and −11–14 PMOs significantly reduced exon 7A inclusion. Although the effect of 1–25 PMO was greater than that of −11–14 PMO, no statistically significant difference was observed between them.

1–25 PMO was so effective at improving alternative splicing of the *Clcn1* minigene in cultured cells that we expected it to work well *in vivo*. To test whether 1–25 PMO could work *in vivo*, we administrated 60 μg of 1–25 PMO intramuscularly four times at weekly intervals into the *tibialis anterior* (TA) muscles of HSA^{LR} mice. The alternative splicing of the *Clcn1* gene was moderately improved, with an approximately 30% decrease in exon 7A inclusion. Electromyography (EMG) with a single needle electrode, however, revealed that the occurrence of myotonia was not altered by PMO injection (Supplementary Fig. S2). Because 60 μg of PMO was quite a high dose for administration into a single muscle, we assumed that an effective delivery system would be required to introduce 1–25 PMO into muscle tissues. We therefore examined the usefulness of ultrasound-enhanced delivery with Bubble liposomes for PMO delivery. We administrated 20 μg of 1–25 PMO three times at weekly intervals into the TA muscles of HSA^{LR} mice with or without Bubble liposomes and ultrasound (Fig. 2). RT-PCR analysis revealed that the rate of inclusion of exon 7A decreased to its lowest level when both Bubble liposomes and ultrasound were applied, indicating that use of the combination of Bubble liposomes and ultrasound could enhance PMO delivery efficiency.

We next investigated whether 1–25 PMO could cure myotonic symptoms in HSA^{LR} mice when delivered using the Bubble liposome-ultrasound system. We administrated 1–25 PMO as described above. Three weeks later, we harvested the injected muscles and conducted RT-PCR and immunohistological analyses. RT-PCR showed that 1–25 PMO decreased the inclusion of exon 7A to a level comparable to that in wild-type FVB/n mice (Fig. 3a). We checked four other alternative splicing events, *Cypher* (*Ldb3*) exon 11, *Mbnl1* exon 5, *Ryr1* exon 70 and *Serca1* exon 22, which are known to be abnormally regulated in patients with DM1and HSA^{LR} mice[30]. We found that the alternative splicing of none of them was changed by

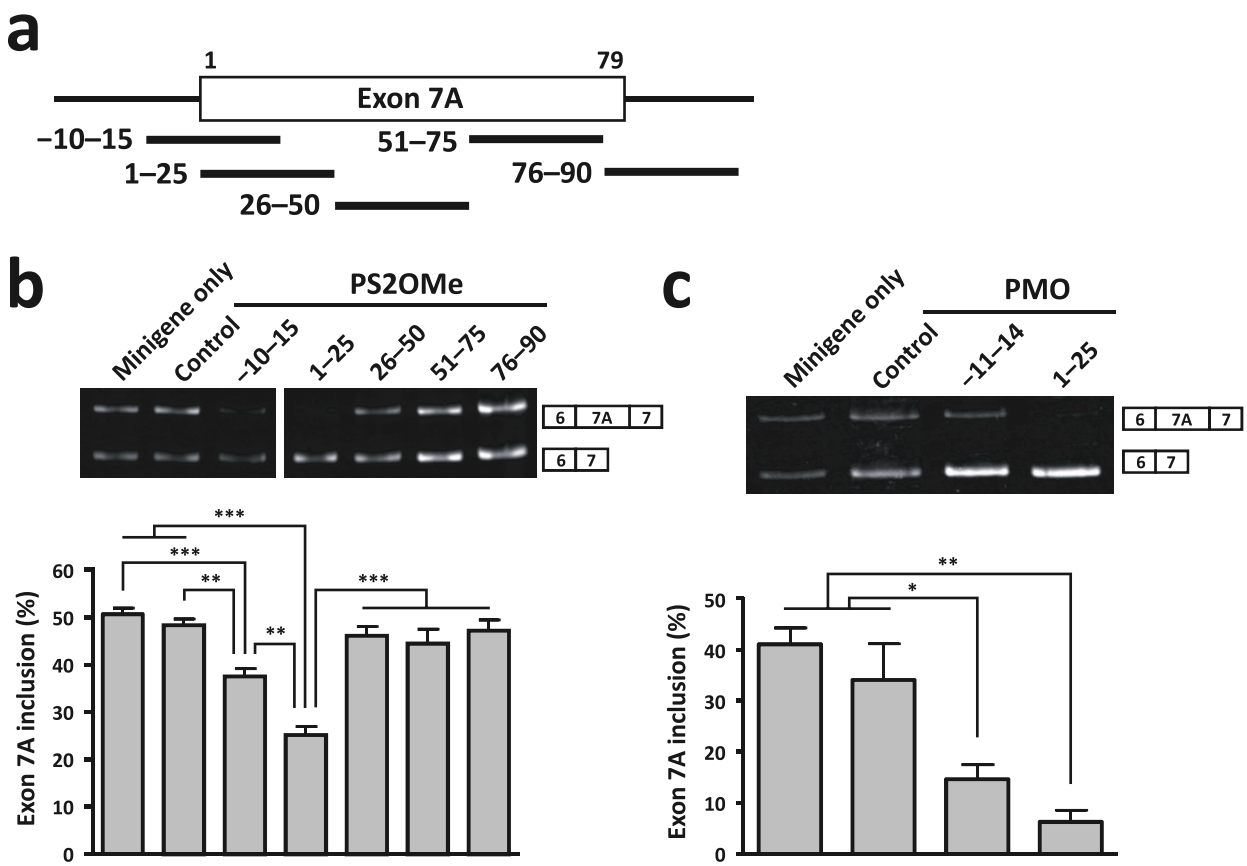

Figure 1 | AON-mediated exclusion of *Clcn1* exon 7A in COS-7 cells. (a) Locations of the target sites of AONs (thick black lines) along the *Clcn1* pre-mRNA. The numbers over exon 7A (rectangle) indicate the positions of nucleotides. (b) Cellular splicing assay to detect the exclusion of exon 7A of the *Clcn1* minigene by PS2OMe RNA in COS-7 cells. 1–25 was the most successful AON. A representative result is shown above and the bars indicate mean and s.e.m. ($n = 6$). (c) The same assay as in (b) except that PMOs were used. 1–25 PMO decreased the inclusion of exon 7A effectively ($n = 3$). Statistical significance was analysed by Tukey's multi-comparison test (* $P < 0.05$, ** $P < 0.01$, *** $P < 0.001$).

the injection of 1–25 PMO (Fig. 3b); thus, the effect of the PMO was specific to the alternative splicing of the *Clcn1* gene.

The abnormal splicing of *Clcn1* is believed to cause myotonia by introducing a premature termination codon into the subsequent exon and by decreasing the expression of the Clcn1 protein via nonsense-mediated mRNA decay. Thus, we examined whether 1–25 PMO restored the expression of Clcn1 protein in HSA^{LR} mice. Immunofluorescence analysis of TA muscles showed the sarcolemmal localisation of Clcn1 protein in wild-type muscle, but such a pattern was not detected in saline-injected HSA^{LR} mice. The injection of 1–25 PMO clearly restored the sarcolemmal distribution, demonstrating that correction of the abnormal splicing of the *Clcn1* gene led to the normal expression of its protein (Fig. 3c).

Finally, we investigated whether injection of 1–25 PMO improved the myotonic phenotype of HSA^{LR} mice. Electromyographic analyses showed bursts of action potentials after electrical stimulation (4–8 V) in HSA^{LR} mice, but not in wild-type mice (Fig. 4a). Myotonia occurred even in denervated muscles (data not shown), which indicates that it was not caused by hyperactivation of motor neurones, but by increased excitability of the sarcolemma. Myotonic EMG activities continued for 1 to 3 s and their average duration was 1.27 s in saline-treated TA muscles. The injection of 1–25 PMO decreased their duration, but the change was not statistically significant; the integrated EMG (iEMG) was reduced by the PMO administration ($P < 0.05$). The decreased iEMG indicated that 1–25 PMO mitigated the hyperexcitability of the HSA^{LR} muscles.

These results suggest that 1–25 PMO could improve the function of the *Clcn1* gene in the DM1 model mouse at the RNA, protein and

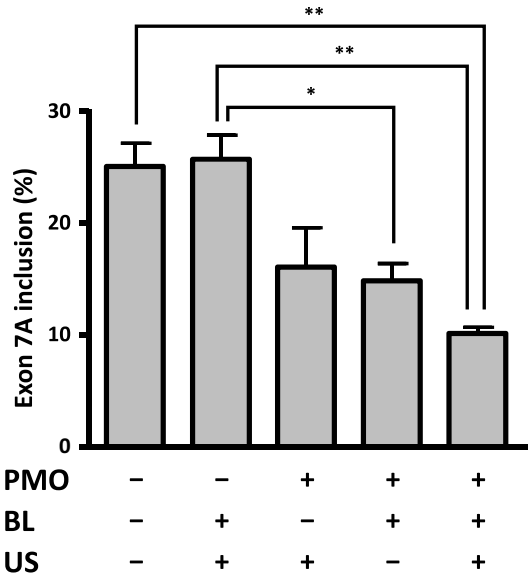

Figure 2 | PMO delivery by the combination of Bubble liposomes and ultrasound. 1–25 PMO (20 μg) or saline was locally administrated into TA muscles of HSA^{LR} mice with/without Bubble liposomes (BLs) and ultrasound (US). The inclusion rate of exon 7A decreased most when both Bubble liposomes and ultrasound were applied. ($n = 3$). The bars indicate mean and s.e.m., and statistical significance was analysed by Tukey's multi-comparison test (* $P < 0.05$, ** $P < 0.01$).

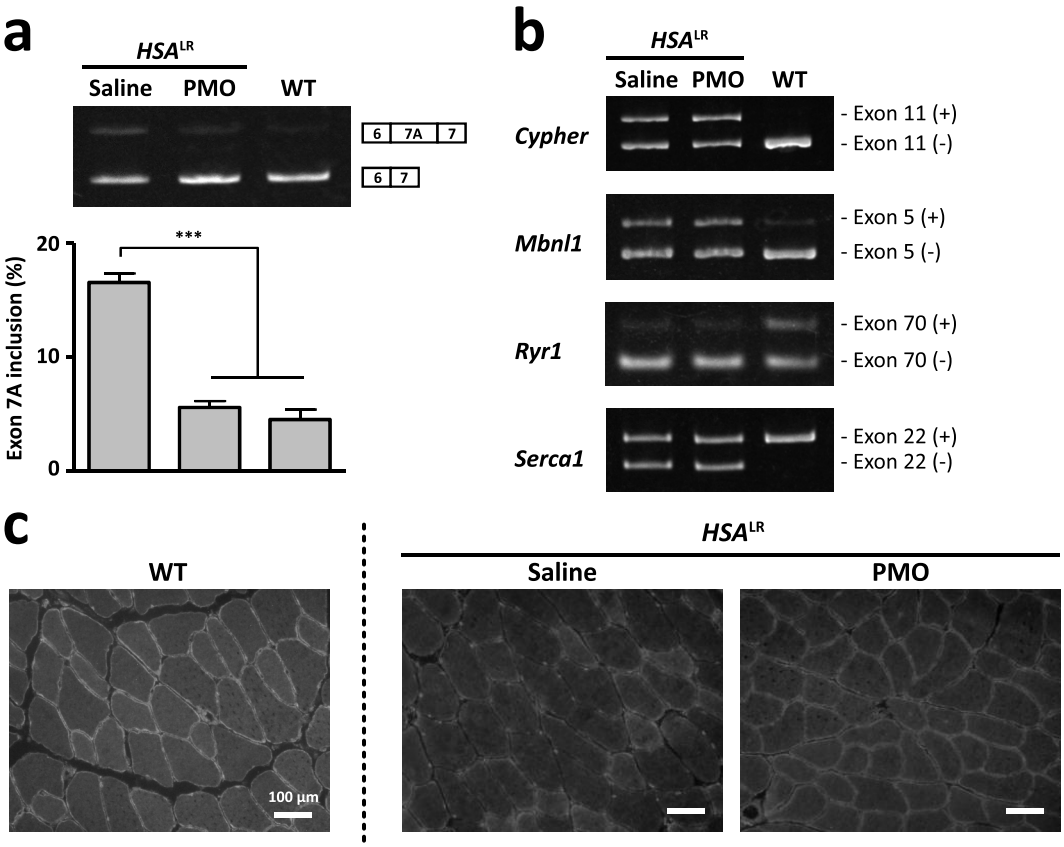

Figure 3 | *In vivo* improvement of aberrant splicing of the *Clcn1* gene by 1–25 PMO. (a) The alternative splicing of *Clcn1* exon 7A in *HSA*^{LR} and WT mice. 1–25 PMO (20 µg) or saline was locally administrated into TA muscles of *HSA*^{LR} mice. The ratio of the splicing variant containing exon 7A in thevPMO-injected muscles decreased to a level comparable with that in WT muscle ($n = 5$). The bars indicate mean and s.e.m., and statistical significance was analysed by Tukey's multi-comparison test (*** $P < 0.001$). (b) Abnormal splicing of other genes in *HSA*^{LR} mice was not affected by 1–25 PMO. (c) Immunofluorescence analysis of transverse sections of TA muscle with an anti-Clcn1 antibody. Injection of 1–25 PMO restored the sarcolemmal localisation of Clcn1 protein in TA muscles of *HSA*^{LR} mice.

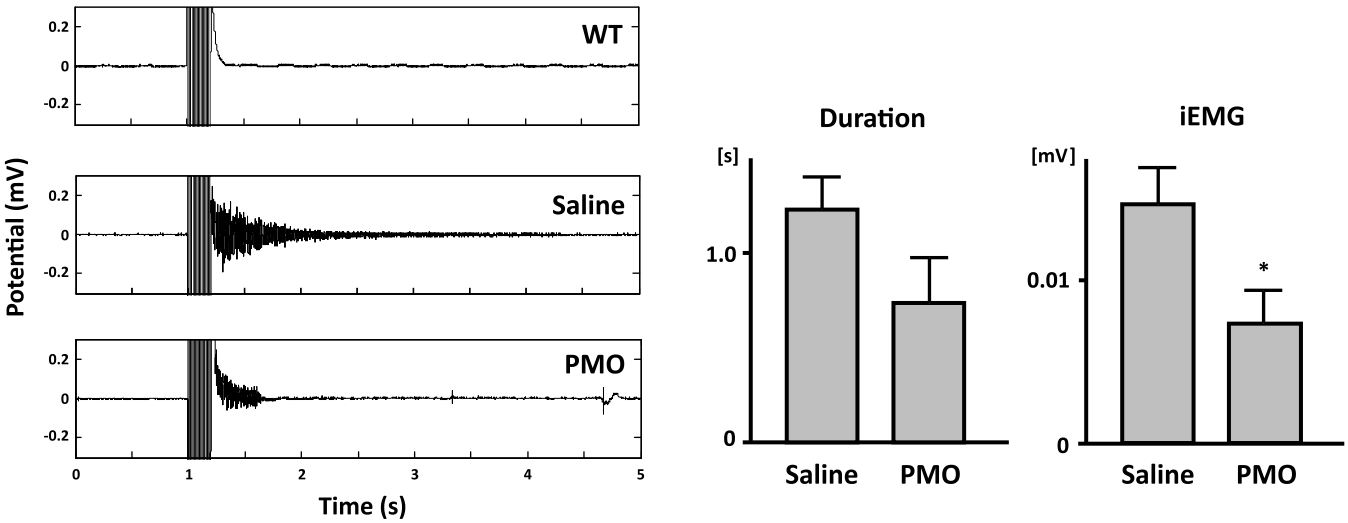

Figure 4 | Reduction of myotonic discharge by 1–25 PMO in *HSA*^{LR} mice. (a) Representative EMG signals of TA muscle. Tibialis muscle was electrically stimulated 1 s after the EMG recording started. In the *HSA*^{LR} muscle, repetitive discharges that were absent in the WT muscle could be seen. (b)vDuration of myotonic discharge and integrated EMG (iEMG). 1–25 PMO significantly reduced iEMG in *HSA*^{LR} muscle (saline, $n = 6$; 1–25 PMO, $n = 7$).The bars indicate mean and s.d., and statistical significance was analysed by Student's *t*-test (* $P < 0.05$).

phenotypic levels, and that the Bubble liposome-ultrasound system should be capable of delivering enough PMO to ameliorate myotonia.

Discussion

The greatest advantage of PMO is its remarkable innocuity. According to a report from Gene Tools, administration of a single 700 mg/kg dose of PMO to a mouse did not cause any obvious acute toxicity[31], while the 50% lethal dose of phosphorothioate DNA, a first-generation antisense oligonucleotide, was estimated to be 750 mg/kg in mice[32]. The high pharmaceutical potential of PMO is also supported by the fact that safety issues were not raised following its administration to mice and humans; however, PMO must overcome the low permeability of the cell membranes to achieve a significant effect on alternative splicing. Because of the inefficient cellular uptake of PMO, systemic delivery and functional splicing modification were not successful in a mouse model[33]. Therefore, for the clinical application of PMO, establishing an effective delivery method is essential.

The major achievement in this study was that we increased the efficiency of PMO delivery using Bubble liposomes and ultrasound. The use of the ultrasound-mediated delivery system with Bubble liposomes improved the alternative splicing of the *Clcn1* gene in *HSA*^{LR} mice to a level comparable to that of wild-type mice and decreased myotonic discharges, indicating that the delivery system increased introduction of 1–25 PMO into skeletal muscle. Our results show that the intramuscular injection itself delivered the PMO into muscle to some extent, and so the intramuscular injection might have contributed to the relief of the pathology. However, the Bubble liposome- and ultrasound-mediated enhancement of delivery efficiency suggests that the new delivery system will have a beneficial effect over much less invasive injection, such as intravenous injection, which cannot by itself be expected to promote the entry of PMO into skeletal muscle[19].

A fair amount of the *Clcn1* splicing variant without exon 7A was expressed even in the *HSA*^{LR} mouse. Because the myotonic discharge of a *HSA*^{LR} mouse was remedied by correcting *Clcn1* alternative splicing in a previous study[14], abnormal splicing of the gene must be the primary cause of myotonia. The expression levels of the "normal" splicing variant in saline-injected muscles were 57% of that in the wild-type muscles. PMO injection increased the expression about 1.4-fold to 78% of that in wild-type mice. As *Clcn1* heterozygous mutant mice did not show a myotonic phenotype[34], the myotonia in *HSA*^{LR} mice was unlikely to have been caused by haploinsufficiency of full-length Clcn1 protein. Instead, the truncated protein translated from the exon 7A-countaining mRNA may have dominant-negative activity, since full-length Clcn1 protein functions in a dimeric form. Berg *et al.* showed that the truncated Clcn1 protein did not function as a chloride channel, but rather disturbed the channel activity of full-length Clcn1 protein[35]. In this study, expression of the splicing variant containing exon 7A was decreased by 40% in the PMO-administered group. Thus, this may have contributed to the improvement of the pathology, as well as the increased expression of the exon 7A skipping variant. The dominant-negative hypothesis suggests that the AON therapy should completely prevent exon 7A inclusion when used to treat myotonia, in contrast to Duchenne muscular dystrophy, in which the partial restoration of dystrophin expression could lead to the improvement of muscle strength.

In the course of our search for the optimal PMO sequence to correct *Clcn1* splicing, we found that 1–25 and 16–40 PMOs suppressed the inclusion of exon 7A well, but that 26–50 PMO did not. The fact that steric blocking of the 16–25 region promoted exon skipping indicates that proteins that bind to this region are essential for exon 7A recognition. Previously, we showed that the 8 nt at the 5′ end of exon 7A serve as an ESE and that an RNA-binding protein, Mbnl1, prevented the inclusion of exon 7A by binding to the ESE[29]. Unlike the ESE, the sequence of the 16–25 region was pyrimidine-rich and did not contain the Mbnl1-recognition motif, YGCY. It remains to be determined which proteins bind to the region to regulate exon 7A splicing.

In this study, we tried to cure DM1 model mice using a PMO targeted to *Clcn1*. However, considering that dozens of genes are abnormally spliced in patients with DM1, it might be impractical to treat all symptoms due to mis-splicing of such genes with AONs at the same time. DM1 is caused by expansion of the CTG repeats in the 3′ UTR region of the DMPK gene. Transcripts with these expanded repeats sequester Mbnl proteins, which regulate alternative splicing, leading to global alternative splicing dysfunction[36]. Thus, expanded CUG repeat-containing RNA must be the most important target of antisense therapy for DM1, and many groups have studied the use of CAG repeat-containing AONs to dissociate Mbnl1 proteins from CUG repeat-containing RNA. Some trials to treat DM1 model mice with CAG AONs were successful[19, 37], but here again the obstacle to clinical application of the AONs was the lack of an efficient delivery method. Our ultrasound-mediated delivery system with Bubble liposomes must have a beneficial effect on the delivery of CAG-containing AONs.

Methods

AONs. Phosphorothioate 2′ *O*-methyl RNA oligonucleotides and phosphorodiamidate morpholino oligonucleotides were purchased from IDT (Coralville, IA, USA) and Gene Tools (Philomath, OR, USA), respectively. The sequences of the oligonucleotides are listed in Supplementary Table ST1. Both AONs were dissolved in water.

Construct. The *Clcn1* minigene has been described previously[29]. Briefly, a *Clcn1* minigene fragment covering exons 6 to 7 was amplified from mouse genomic DNA by PCR and inserted into the *Bgl*II-*Sal*I sites of pEGFP-C1 (Clontech Laboratories, Mountain View, CA, USA).

Cellular splicing assay. COS-7 cells were cultured in Dulbecco's modified Eagle's medium (DMEM; Sigma-Aldrich, St. Louis, MO, USA) supplemented with 10% heat-inactivated fetal bovine serum (Life Technologies, Foster City, CA, USA) in a humidified atmosphere containing 5% CO_2 at 37°C.

For the splicing assay, COS-7 cells were cultured in 12-well plates and transfected with 0.1 μg of the *Clcn1* minigene and AONs (0.1 μmol) at 60–80% confluence. Polyethylenimine and Endo-Porter (Gene Tools) were used for the transfection of PS2OMe RNA and PMOs, respectively. Forty-eight hours later, total RNA was extracted from the transfected cells using a GenElute Mammalian Total RNA Miniprep Kit (Sigma-Aldrich).

Animals. *HSA*^{LR} mice are FVB/n-background transgenic mice that express expanded CTG repeats under the control of the human skeletal actin promoter in skeletal muscle[38]. Compared with the first established line, the number of the repeat was reduced: the mice used in this study carried 180–200 repeats. All the mutant mice showed persistent contraction of gluteal muscles after they bucked. We used FVB/nJcl mice (Clea Japan, Tokyo, Japan) as wild-type controls.

The present study was approved by the Ethical Committee for Animal Experiments at the University of Tokyo, and was carried out in accordance with the Guidelines for Research with Experimental Animals of the University of Tokyo and the NIH Guide for the Care and Use of Laboratory Animals (NIH Guide, revised 1996).

Bubble liposomes. Bubble liposomes were prepared by previously described methods[24]. Briefly, PEG liposomes composed of 1,2-dipalmitoyl-sn-glycero-3-phosphocholine (DPPC) (NOF Corporation, Tokyo, Japan) and 1,2-distearoyl-sn-glycero-3-phosphatidyl-ethanolamine-polyethyleneglycol (DSPE-PEG2000-OMe) (NOF Corporation) at a molar ratio of 94 : 6 were prepared by a reverse phase evaporation method. Briefly, all reagents were dissolved in 1 : 1 (v/v) chloroform/diisopropyl ether. Phosphate-buffered saline was added to the lipid solution, and the mixture was sonicated and then evaporated at 47°C. The organic solvent was completely removed, and the size of the liposomes was adjusted to less than 200 nm using extruding equipment and a sizing filter (pore size: 200 nm) (Nuclepore Track-Etch Membrane; Whatman Plc, Maidstone, Kent, UK). The lipid concentration was measured using a Phospholipid C test (Wako Pure Chemical Industries, Ltd, Osaka, Japan). Bubble liposomes were prepared from liposomes and perfluoropropane gas (Takachio Chemical Ind. Co. Ltd, Tokyo, Japan). First, 2-ml sterilised vials containing 0.8 ml of liposome suspension (lipid concentration: 1 mg/ml) were filled with perfluoropropane gas, capped and then pressurised with a further 3 ml of perfluoropropane gas. The vial was placed in a bath-type sonicator (38 kHz, 250 W) (SONO-CLEANER CA-4481L; Kaijo Denki, Tokyo, Japan) for 1 min to form Bubble liposomes.

Injection of morpholino oligonucleotides with Bubble liposomes and ultrasound. PMO (20 μg) and the Bubble liposome suspension (30 μl) were injected into the TA muscles of *HSA*^{LR} mice (6 weeks old) using a 30-gauge needle (NIPRO Co., Osaka, Japan). Immediately after injection, ultrasound (frequency, 1 MHz; duty, 50%; intensity, 2.0 W/cm^2; time, 60 s) was applied transdermally downstream of the injection site using a 6-mm diameter probe. A SONITRON 1000 device (Rich-Mar, Chattanooga, TN, USA) was used to generate the ultrasound. We administrated the PMO three times at weekly intervals. Three weeks after the last administration, we performed EMG measurements and then killed the mice and harvested the TA muscles for RT-PCR analysis and immunohistochemistry.

Electromyographic recording and electrical stimulation. Implantation of EMG electrodes and stimulating electrodes was carried out under aseptic conditions on mice anaesthetised with 2% vapourised isoflurane in air. Body temperature was measured rectally and was maintained at 37–38°C using a homeothermic heating pad (BioResearch Center, Aichi, Japan). Bipolar wire electrodes (tip distance, 1–2 mm) made of Teflon-insulated stainless steel wire (76 μm diameter bare, 140 μm coated; cat. no. 791000; A-M Systems, Carlsborg, WA, USA) were implanted in the TA and gastrocnemius (GA) muscles to record EMG activity. The electrical stimulation of the TA muscle was achieved using two wire electrodes that were inserted under the skin over the TA muscle and placed along the longitudinal axis of the muscle. After full recovery from the anaesthesia, alert mice were restrained in a cylindrical mouse-sized cage, with their hind limbs out of the cage to maintain their muscles at their resting lengths. The EMG signals were amplified and bandpass filtered (15 Hz–1 KHz; AB-611J; Nihon-Koden, Co., Tokyo, Japan), digitised with an analog-digital converter (PowerLab 16/30, ADInstruments Ltd, Oxford, UK) and recorded (sampling rate 10 kHz) on a computer. Electrical stimulation consisted of repetitive square pulses (train of 20 pulses at 100 Hz, 1 ms duration) delivered by an isolation unit (SS-202J; Nihon-Koden) connected to a pulse generator (SEN-3401, Nihon-Koden). The stimulus intensity was adjusted to evoke ankle dorsiflexion and avoid overt movements and animal discomfort. EMG measurements were recorded in single-blinded manner.

EMG data analysis. Myotonic EMG activities were easily confirmed by visual inspection and analysed using custom-written MATLAB software (MathWorks, Inc., Natick, MA, USA). EMG signals were full-wave-rectified and filtered with a 20 Hz low-pass second-order Butterworth filter. Offset of the EMG signal was defined as a deflection below three standard deviations from baseline. The baseline level was defined as the mean EMG signal in the resting state before stimulation. Duration of myotonic activities was defined as the period from the termination of stimulation to the offset time. Myotonic activities were integrated during the duration of myotonia and calculated by subtracting the baseline level. To quantify EMG activities per unit time, iEMG values were then calculated as the integrated myotonia value divided by corresponding net duration. The EMG data were analysed in a single-blinded manner.

RT-PCR analysis. Total RNA was extracted from TA muscles and cultured cells using TRIzol reagent (Life Technologies) and a GenElute Mammalian Total RNA Miniprep Kit (Sigma-Aldrich), respectively, according to the manufacturers' instructions.

Typically, 0.5–1.0 μg of total RNA was reverse-transcribed with a PrimeScript 1st Strand cDNA Synthesis Kit (Takara Bio, Shiga, Japan) using oligo(dT) primers. PCR reactions were performed using Ex Taq DNA polymerase (Takara Bio). The sequences of the PCR primers are listed in Supplementary Table ST2. The products were electrophoretically resolved on an 8% polyacrylamide gel that was stained with ethidium bromide and analysed using an LAS-3000 luminescence image analyser (FujiFilm, Tokyo, Japan). The ratio of exon 7A inclusion in *Clcn1* mRNA was calculated as (7A inclusion)/(7A inclusion + 7A skipping) × 100.

Immunofluorescence. Frozen sections (6 μm thick) of unfixed TA muscles were immunostained with an affinity-purified rabbit polyclonal anti-Clcn1 antibody (dilution 1 : 50; Alpha Diagnostics International, San Antonio, TX, USA). The secondary antibody was Alexa Fluor 488-conjugated goat anti-rabbit IgG (Life Technologies) used at a dilution of 1 : 600. Images were collected using an IX70 inverted microscope (Olympus, Tokyo, Japan) equipped with a ×20 objective lens. Exposure time and threshold were identical for all comparisons of antisense and saline controls.

Statistics. A two-tailed Student's *t*-test or Tukey's multiple comparison test were used for statistical comparison.

1. Aslanidis, C. *et al.* Cloning of the essential myotonic dystrophy region and mapping of the putative defect. *Nature* **355**, 548–551 (1992).
2. Brook, J. D. *et al.* Molecular basis of myotonic dystrophy: expansion of a trinucleotide (CTG) repeat at the 3′ end of a transcript encoding a protein kinase family member. *Cell* **68**, 799–808 (1992).
3. Buxton, J. *et al.* Detection of an unstable fragment of DNA specific to individuals with myotonic dystrophy. *Nature* **355**, 547–548 (1992).
4. Harley, H. G. *et al.* Expansion of an unstable DNA region and phenotypic variation in myotonic dystrophy. *Nature* **355**, 545–546 (1992).
5. Harper, P. S. *Myotonic dystrophy,* 3rd ed. (Saunders, W. B. Philadelphia, 2001).
6. Philips, A. V., Timchenko, L. T. & Cooper, T. A. Disruption of splicing regulated by a CUG-binding protein in myotonic dystrophy. *Science* **280**, 737–741 (1998).
7. Savkur, R. S., Philips, A. V. & Cooper, T. A. Aberrant regulation of insulin receptor alternative splicing is associated with insulin resistance in myotonic dystrophy. *Nat. Genet.* **29**, 40–47 (2001).
8. Fugier, C. *et al.* Misregulated alternative splicing of BIN1 is associated with T tubule alterations and muscle weakness in myotonic dystrophy. *Nat. Med.* **17**, 720–725 (2011).
9. Koebis, M. *et al.* Alternative splicing of myomesin 1 gene is aberrantly regulated in myotonic dystrophy type 1. *Genes Cells* **16**, 961–972 (2011).
10. Ohsawa, N., Koebis, M., Suo, S., Nishino, I. & Ishiura, S. Alternative splicing of PDLIM3/ALP, for alpha-actinin-associated LIM protein 3, is aberrant in persons with myotonic dystrophy. *Biochem. Biophys. Res. Commun.* **409**, 64–69 (2011).
11. Charlet, B. N. *et al.* Loss of the muscle-specific chloride channel in type 1 myotonic dystrophy due to misregulated alternative splicing. *Mol. Cell.* **10**, 45–53 (2002).
12. Mankodi, A. *et al.* Expanded CUG repeats trigger aberrant splicing of ClC-1 chloride channel pre-mRNA and hyperexcitability of skeletal muscle in myotonic dystrophy. *Mol. Cell.* **10**, 35–44 (2002).
13. Lossin, C. & George, A. L. Jr. Myotonia congenita. *Adv. Genet.* **63**, 25–55 (2008).
14. Wheeler, T. M., Lueck, J. D., Swanson, M. S., Dirksen, R. T. & Thornton, C. A. Correction of ClC-1 splicing eliminates chloride channelopathy and myotonia in mouse models of myotonic dystrophy. *J. Clin. Invest.* **117**, 3952–3957 (2007).
15. Kole, R., Krainer, A. R. & Altman, S. RNA therapeutics: beyond RNA interference and antisense oligonucleotides. *Nat. Rev. Drug. Discov.* **11**, 125–140 (2012).
16. Stein, D., Foster, E., Huang, S. B., Weller, D. & Summerton, J. A specificity comparison of four antisense types: morpholino, 2′-O-methyl RNA, DNA, and phosphorothioate DNA. *Antisense Nucleic Acid Drug Dev.* **7**, 151–157 (1997).
17. Wu, B. *et al.* Dose-dependent restoration of dystrophin expression in cardiac muscle of dystrophic mice by systemically delivered morpholino. *Gene Ther.* **17**, 132–140 (2010).
18. Wheeler, T. M. *et al.* Targeting nuclear RNA for in vivo correction of myotonic dystrophy. *Nature* **488**, 111–115 (2012).
19. Leger, A. J. *et al.* Systemic delivery of a peptide-linked morpholino oligonucleotide neutralizes mutant RNA toxicity in a mouse model of myotonic dystrophy. *Nucleic Acid Ther.* **23**, 109–117 (2013).
20. Lu, Q. L., Liang, H. D., Partridge, T. & Blomley, M. J. Microbubble ultrasound improves the efficiency of gene transduction in skeletal muscle in vivo with reduced tissue damage. *Gene Ther.* **10**, 396–405 (2003).
21. Shen, Z. P., Brayman, A. A., Chen, L. & Miao, C. H. Ultrasound with microbubbles enhances gene expression of plasmid DNA in the liver via intraportal delivery. *Gene Ther.* **15**, 1147–1155 (2008).
22. Haag, P. *et al.* Microbubble-enhanced ultrasound to deliver an antisense oligodeoxynucleotide targeting the human androgen receptor into prostate tumours. *J. Steroid Biochem. Mol. Biol.* **102**, 103–113 (2006).
23. Suzuki, R. *et al.* Gene delivery by combination of novel liposomal bubbles with perfluoropropane and ultrasound. *J. Control Release* **117**, 130–136 (2007).
24. Negishi, Y. *et al.* Delivery of an angiogenic gene into ischemic muscle by novel bubble liposomes followed by ultrasound exposure. *Pharm. Res.* **28**, 712–719 (2011).
25. Negishi, Y. *et al.* Local gene delivery system by bubble liposomes and ultrasound exposure into joint synovium. *J. Drug Deliv.* **2011**, 203986 (2011).
26. Negishi, Y. *et al.* Systemic delivery systems of angiogenic gene by novel bubble liposomes containing cationic lipid and ultrasound exposure. *Mol. Pharm.* **9**, 1834–1840 (2012).
27. Sugano, M. *et al.* Gene delivery system involving Bubble liposomes and ultrasound for the efficient in vivo delivery of genes into mouse tongue tissue. *Int. J. Pharm.* **422**, 332–337 (2012).
28. Negishi, Y. *et al.* AG73-modified Bubble liposomes for targeted ultrasound imaging of tumor neovasculature. *Biomaterials* **34**, 501–507 (2013).
29. Kino, Y. *et al.* MBNL and CELF proteins regulate alternative splicing of the skeletal muscle chloride channel CLCN1. *Nucleic Acids Res.* **37**, 6477–6490 (2009).
30. Lin, X. *et al.* Failure of MBNL1-dependent post-natal splicing transitions in myotonic dystrophy. *Hum. Mol. Genet.* **15**, 2087–2097 (2006).
31. Summerton, J. & Weller, D. Morpholino antisense oligomers: design, preparation, and properties. *Antisense Nucleic Acid Drug Dev.* **7**, 187–195 (1997).
32. Templeton, N. S. & Templeton, N. S. *Gene and cell therapy: therapeutic mechanisms and strategies.* 2nd ed. (Marcel Dekker, New York, 2004).
33. Sazani, P. *et al.* Systemically delivered antisense oligomers upregulate gene expression in mouse tissues. *Nat. Biotechnol.* **20**, 1228–1233 (2002).
34. Chen, M. F., Niggeweg, R., Iaizzo, P. A., Lehmann-Horn, F. & Jockusch, H. Chloride conductance in mouse muscle is subject to post-transcriptional compensation of the functional Cl- channel 1 gene dosage. *J. Physiol.* **504**, 75–81 (1997).
35. Berg, J., Jiang, H., Thornton, C. A. & Cannon, S. C. Truncated ClC-1 mRNA in myotonic dystrophy exerts a dominant-negative effect on the Cl current. *Neurology* **63**, 2371–2375 (2004).
36. Ranum, L. P. & Cooper, T. A. RNA-mediated neuromuscular disorders. *Annu. Rev. Neurosci.* **29**, 259–277 (2006).

37. Wheeler, T. M. *et al.* Reversal of RNA dominance by displacement of protein sequestered on triplet repeat RNA. *Science* **325**, 336–339 (2009).
38. Mankodi, A. *et al.* Myotonic dystrophy in transgenic mice expressing an expanded CUG repeat. *Science* **289**, 1769–1773 (2000).

Acknowledgements

We thank Prof. Charles A. Thornton (University of Rochester) for providing us *HSA*^{LR} mice. We also thank Dr H. Mitsuhashi for valuable discussions and encouragement. This work was supported in part by the Comprehensive Research on Disability Health and Welfare, from the Ministry of Health, Labour and Welfare Japan, and Intramural Research Grant (23–5) for Neurological and Psychiatric Disorders of NCNP.

Author contributions

S.I. conceived the project. M.K. designed the experiments. T.K. carried out cell culture-based splicing assay. K.N., M.P.T. carried out the delivery of PMO. R.M., Y.H. and I.N. carried out histochemical staining. H.Y., M.H., M.S. and D.Y. designed and carried out EMG analysis. Y.N. and Y.E.-T. prepared Bubble liposomes.

Additional information

Supplementary Information accompanies this paper at http://www.nature.com/scientificreports

Competing financial interests: The authors declare no competing financial interests.

How to cite this article: Koebis, M. *et al.* Ultrasound-enhanced delivery of Morpholino with Bubble liposomes ameliorates the myotonia of myotonic dystrophy model mice. *Sci. Rep.* **3**, 2242; DOI:10.1038/srep02242 (2013).

This work is licensed under a Creative Commons Attribution-NonCommercial-NoDerivs 3.0 Unported license. To view a copy of this license, visit http://creativecommons.org/licenses/by-nc-nd/3.0